Available online at www.sciencedirect.com
SCIENCE DIRECT®
PERGAMON
Continental Shelf Research 23 (2003) 177–191
CONTINENTAL SHELF RESEARCH
www.elsevier.com/locate/csr

Autumnal reduction of stratification in the northern North Sea and its impact

Hans van Haren[a,*], M.J. Howarth[b], K. Jones[c], I. Ezzi[c]

[a] *Netherlands Institute for Sea Research (NIOZ), P.O. Box 59, 1790 AB Den Burg, The Netherlands*
[b] *Proudman Oceanographic Laboratory, Bidston Observatory, Birkenhead, Merseyside, CH43 7RA, UK*
[c] *Dunstaffnage Marine Laboratory, P.O. Box 3, Oban, Argyll PA34 4AD, UK*

Accepted 7 September 2002

Abstract

In the autumn vertical density stratification in the northern North Sea is reduced primarily by atmospheric induced mixing. However, observations from moored instruments show that a sudden enhanced exchange of nutrients from the light-limited, nutrient-rich deep layer into the nutrient-depleted near-surface layer occurred *indirectly* when inertial shear was largest, across the stratification. An associated response in phytoplankton biomass was not observed, perhaps because the observations were stopped before a proper response could occur. In general, phytoplankton were observed to vary strongly with stratification close to the surface.

Different methods for observing stratification are compared—vertical current shears inferred from Acoustic Doppler Current Profiler data are a good indicator of layers of enhanced stratification, whereas the back-scattered amplitude data from the same instrument are not. The latter data are also found not to be a good indicator for suspended sediment, despite extensive reworking of the bottom at 110 m depth due to the action of surface waves. The observed enhancement of the turbulent bottom boundary layer exceeding the tidal frictional layer is discussed, when stratification is still enhanced near mid-depth.

Keywords: Stratification; Shear; Autumn; Nutrients; Northern North Sea; 59°N 01°E

1. Introduction

In this paper, we examine the mechanisms resulting in the variations of the strength of vertical stratification in density with depth and time and the effects on the vertical exchange of material, exemplified by nutrients. Within the European Community funded MAST3 program 'Processes of Vertical Exchange in Shelf Seas' (PROVESS), the time evolution of stratification was monitored using two months of temperature and acoustic Doppler current profiler (ADCP) observations from a 110 m deep mooring site in the northern North Sea. At this site weakly stratified near-surface and near-bottom boundary layers do not overlap until very late in autumn (Fig. 1).

When atmospheric induced mixing by wind stress or convective overturning is larger than heating by solar insolation, the gradual increase of

*Corresponding author.
E-mail address: hansvh@nioz.nl (H. van Haren).

0278-4343/03/$ - see front matter
PII: S0278-4343(02)00171-1

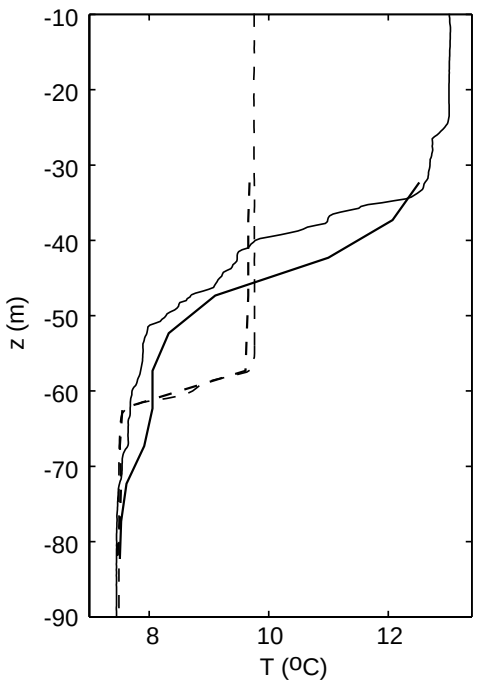

Fig. 1. Examples of observed vertical profiles of temperature near the beginning (day 253; solid line) and end (300; dashed line) of the mooring period at the central PROVESS northern North Sea site. Curves starting at 33 m depth are from the thermistor string, while the others are from CTD. Note the strong variation with time of the pycnocline depth, as none of the profiles were obtained at exactly the same moment. Time is given in yeardays, according to the PROVESS-convention that yearday 1.5 = 12.00 UTC at January 1.

density with depth becomes concentrated in a 'pycnocline' at some depth below the surface with a near-homogeneous ('mixed') layer above. However, static stable density stratification limits turbulent mixing and hence further deepening (erosion) of the pycnocline. Furthermore, the wind stress response distribution in the ocean is affected by the rotation of the earth, resulting in an 'Ekman layer' of (rotating) current shear stress of limited vertical extent. Pollard et al. (1973) show that pycnocline deepening following a wind stress (τ) increase is arrested after one inertial period $t_f = 2\pi/f$, where f denotes the local inertial frequency, reaching an Ekman layer depth of $h_s \propto (|\tau|/\rho f N)^{0.5} \approx 25$ m for typical values of stratification or buoyancy frequency N and density ρ. This is comparable to a typical depth of near-surface mixing caused by (nighttime) cooling (Brainerd and Gregg, 1995).

As a result, limited pycnocline deepening is often modeled as an *externally* governed turbulent erosion process. For shallow seas like the central North Sea, where it may be arrested by (tidal) friction from below, the result is an extremely sharp pycnocline near mid-depth (van Haren, 2000). However, Pollard et al. (1973) also argue that extended pycnocline deepening is related to a Richardson number, which describes the balance between stable density stratification and the eroding turbulent friction velocity. In this paper, we interpret turbulence within a pycnocline as an *internal* mixing process, following Krauss (1981) and his interpretation of observations made in the Baltic Sea in autumn.

Krauss showed pycnocline erosion was caused by transient inertial currents following the passage of an atmospheric disturbance and could be modeled using time-dependent Ekman solutions. Inertial motions have the peculiar behavior of being only generated because of the reduced level of turbulent viscosity within the pycnocline, so that the near-surface layer acts like a slab (Pollard and Millard, 1970). As a result, large inertial current differences ('shear') are observed across the pycnocline, which may enhance mixing locally. Essentially, Krauss' observations showed a strong thickening of the pycnocline when inertial motions were generated. Such thickening indicates mixing across the pycnocline, which however, was observed arrested after an inertial period, expressing the typical timescale of the subtle balance setup between shear and stratification (van Haren, 2000). Identical observations have been reported throughout the seasonal cycle of stratification in the central North Sea, in spring (van Haren, 2000), summer (van Haren et al., 1999) and autumn (van Haren, 1996).

We present a comprehensive set of observations including a diagnostic of mixing across the pycnocline, in the form of a rare time series of nutrients. In addition to the observations by Krauss (1981), modern equipment allows more details that show occasionally a different response of initially *thinning* of the pycnocline following

enhanced inertial shear, otherwise confirming the importance of inertial motions for diapycnal exchange. Similar observations in the stratified central North Sea are used for comparison. Typical observations for the northern North Sea are already visible in a simple diagram like Fig. 1. There, the initially broad pycnocline not only thins following decreasing near-surface temperatures when time progresses, but also implies enhancement of friction at the bottom before stratification is entirely removed and before turbulence fills the entire water column.

2. Data

We report on some observations made in the northern North Sea, where an array of moorings was deployed halfway between northern Scotland and southern Norway (Fig 2) from 10 September–3 November, 1998. The water depth, H, was 110 m, and the bottom topography varied with typical values for large scale variations $|\mathrm{d}H/\mathrm{d}x| \approx |\mathrm{d}H/\mathrm{d}y| \approx 1-2\times10^{-3}$ over horizontal distances of O (10 km).

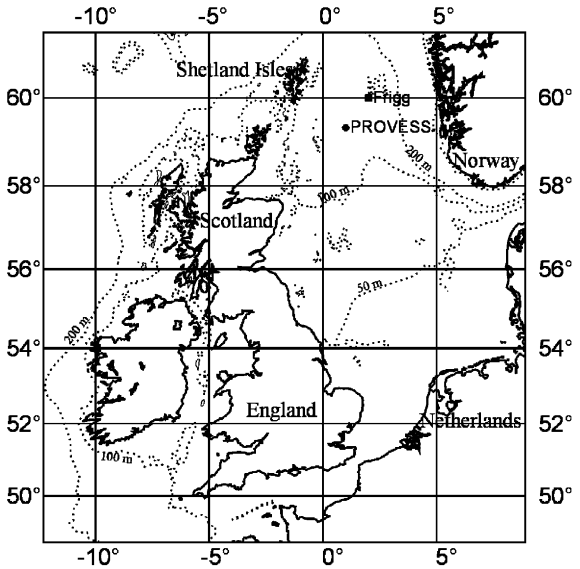

Fig. 2. Map of the North Sea showing the PROVESS' northern mooring site and oilrig 'Frigg' at which meteorological data were collected.

A 150 kHz RDI-broadband ADCP was deployed in a sea bed frame at 59°20′N, 01°00′E ($f=1.25\times10^{-4}\,\mathrm{s}^{-1}$). Throughout, frequency is expressed in s^{-1} ($=86400/2\pi$ cpd, cycle per day). The ADCP sampled 10 min averaged data in 30 vertical bins of 4 m each from 11 m above the bottom to well above the surface. Useful horizontal current data unspoiled by sidelobe returns from the surface ranged from 11 to 88 m depth.

Timeseries of dissolved nutrients were made using a WS-Oceans Ltd NAS-2E in situ nitrate auto-analyzer mounted at a depth of 1.5 m, below a surface buoy moored 2 km from the ADCP. The NAS sampled once every 2 h from its surrounding waters, except when an onboard standard sample was taken (every 6th). Chelsea Instruments Aquatracka in situ fluorometers were moored at 1.5, 15 and 60 and 99 m depth, sampling hourly (15 m) or two-hourly. A standard Aanderaa thermistor string was moored about 5 km from the ADCP. It sampled temperature every 5 min at its 11 thermistors separated by 5 m vertically, the lowest being 26 m above the bottom.

Meteorological data were sampled at a surface buoy at the mooring site, but most of the sensors broke down during the first severe storm in early October. Instead, meteorological data from the Frigg oilrig (59°54′N, 02°06′E) are used. For unknown reasons the wind speed data had to be multiplied by a factor of 1.25, as appeared after comparison with ships' data (Knight et al., 2002).

Shortly after deployment and during the last two weeks before the recovery of the moorings, 24 Hz sampling Seabird SBE-911 CTD and CTD-Rosette information were obtained for calibration purposes and for detailed information resolving almost the entire water column. A total of about 100 profiles were obtained, randomly distributed over the above periods.

3. Methods

3.1. Defining stratification, shear and mixing observables

The limited CTD-information was used to establish the relationship between variations in

density (ρ, in kg m^{-3}) and temperature (T, in °C) in the main pycnocline, since salinity contributes substantially to density variations.

$$\delta\rho = -(0.20 \pm 0.05)\delta T,\ n = 64,\ \text{yearday}[255, 260], \tag{1a}$$

$$\delta\rho = -(0.25 \pm 0.02)\delta T,\ n = 42,\ \text{yearday}[290, 300], \tag{1b}$$

where n indicates the number of CTD casts over which average density–temperature relationships are established. Clearly, this relationship is not very tight over the two months period, albeit shorter periods of 1–2 weeks show consistent relationships. Essentially, the standard deviations in the practical definition (1) reflect temperature (depth) dependence. Using day 280 during the strong decrease of surface temperature as transition day for the two definitions, Eq. (1a) is invoked to convert thermistor string data to time-depth series of stratification, in terms of the static stable buoyancy frequency,

$$N(z,t) = \left(-g\frac{\mathrm{d}\ln\rho}{\mathrm{d}z}\right)^{0.5}, \tag{2}$$

where g denotes acceleration of gravity. N differs by 10% using relationships (1a) and (1b).

The intention is to observe the *dynamical* stability of the water column from the gradient Richardson number,

$$Ri(z,t) = \frac{N^2}{|\mathbf{S}|^2}, \tag{3}$$

as the ratio of static stability and the magnitude of the de-stabilizing vertical current shear vector,

$$\mathbf{S}(z,t) = \left(\frac{\partial u}{\partial z}, \frac{\partial v}{\partial z}\right), \tag{4}$$

where u, v denote the horizontal current components. The quantities in Eqs. (2)–(4) are slowly varying functions with respect to variations of the motions they are generating, guiding or de-stabilizing, such as turbulence and high-frequency internal waves.

Using information from observations made in the central North Sea in 1994, northern North Sea data from the ADCP and thermistor string are used to compute Ri in Eq. (3). Although the instruments were 5 km apart, this is justified because shear at the inertial frequency is dominant, so that its vector describes a circular path and its magnitude varies on a much slower timescale than individual components (van Haren, 2000). Then, with caution and noting the relatively crude vertical resolution of the instruments, horizontal variations in stratification and shear are equivalently assumed relatively small on (sub-)inertial scales. Whether the above assumptions are correct and whether they describe the shear-stratification relationship to first order will be verified.

In the central North Sea, both the layers of enhanced stratification and of shear are found to be about equal in thickness (van Haren, 2000). The observed average gradient Richardson number,

$$Ri(D, t > t_f) = c \approx 0.5 - 1.0, \tag{5}$$

in the layers of largest N, within the thickness D of the pycnocline *and* the enhanced shear layer, c being a constant. This Ri-value is above the critical value for linear stability of small disturbances ($Ri = 0.25$), but below the value $Ri = 1$ for "formal stability" considering three-dimensional nonlinear stratified flows (Miles, 1987). Thus, we want to verify whether similar 'marginal dynamical stability' conditions also apply for the northern North Sea.

As laboratory experiments show that an indication of ongoing mixing within the layers of enhanced shear and stratification is given by their having the same thickness (Linden, 1979), one may monitor these layer thicknesses in addition to verifying Eq. (5). In practice, the variation with time of the thickness of the pycnocline D is defined as,

$$D(t) = h_s - h_b, \tag{6}$$

with weakly stratified layers,

$h_s(t) = z_1(T_1 - T_s > 0.1^\circ C, t)$, near the surface and,

$h_b(t) = z_2(T_2 - T_b < 0.1^\circ C, t)$, near the bottom.

T_s and T_b denote temperatures measured as close as possible to the surface and the bottom, respectively. Similarly, thickness of the shear layer D^S away from surface and bottom boundaries is

defined as,

$$D^S(t) = h_s^S - h_b^S, \quad (7)$$

provided they are separated from the shear at surface and bottom by weakly sheared layers,

$$h_s^S(t) = z_1(|\mathbf{S}|_1 > 0.006\,\mathrm{s}^{-1}, t), \text{ for } z \downarrow z_1 > -20\,\mathrm{m},$$

$$h_b^S(t) = z_2(|\mathbf{S}|_2 > 0.006\,\mathrm{s}^{-1}, t), \text{ for } z \uparrow z_2 > -H + 20\,\mathrm{m}.$$

All transition values in Eqs. (6) and (7) are arbitrary, albeit based on the instruments' accuracies and on typical values for the extent of the surface and bottom boundary shear stress. The latter (taken as 20 m here), especially, are subject to adjustment in special cases, such as during storms but also during very calm weather when mixing layers tend to be small. In terms of stratification (2) and invoking *Ri* in Eqs. (3) and (5), the (temperature) transition value in Eq. (6) corresponds to the shear transition value in Eq. (7), when a typical vertical length scale of 5 m is used.

To quantify the effects of marginal stability across enhanced stratification, turbulent diffusivity $K(z)$ was estimated from CTD-observations by tracking small-scale overturning instabilities from the raw data resolved to 10 cm on average in the vertical. Following Thorpe (1987):

$$K = 0.15 d^2 N, \quad (8)$$

where d indicates the vertical distance over which the instability has to be displaced to obtain a 're-ordered' entirely static stable density profile. As N is extremely difficult to estimate properly in the weakly stratified surface and bottom boundary layers, Eq. (8) is only used to estimate $K(z)$ across the pycnocline using a condition $N(z) > N_m = 0.006\,\mathrm{s}^{-1}$, a relatively high (arbitrary) minimum value, but similar to the transition value in Eq. (7).

3.2. Some additional ADCP observables

Apart from horizontal current components and associated vertical current shear, ADCP data are used to infer the depth-time variation of stratification by monitoring the amplitude of the back-scattered echo ('echo intensity', I) and to monitor the effects of surface waves using above-surface echo intensity (I_a). Details of methods are given in van Haren (2001).

Raw-I are expressed in decibels (dB) after correction for the attenuation of sound in water by referencing them to a minimum value in the record at each depth level, which is adjusted and smoothed using theoretical information from rather imprecise formulae as in Gordon (1996). These formulae contain unknowns such as the source level of energy, and the attenuation coefficients per frequency band vary by up to 10%. The result is a series of data in which in a relative sense all variation is due to different materials in suspension, 'heard' differently by an ADCP. Well known are scatterers like air bubbles entrained near the surface, zooplankton species migrating up and down the water column daily and sediment brought in suspension through bottom friction. Echo intensity data sampled outside the maximum ranges of sea surface waves are proportional to wind stress and wave height (van Haren, 2001).

3.3. Calibrating in-situ nutrient and fluorescence measurements

Calibration of NAS-2E nutrients was achieved by measuring the response to an internal nitrate standard ($10\,\mu\mathrm{mol}\,\mathrm{l}^{-1}\mathrm{NO_3}$–N), every sixth sample. Additionally, recorded values of nitrate concentration in surrounding water were validated by analysing water samples obtained at the beginning and at the end of the mooring period period using flow injection techniques described in Hill et al. (1998).

Fluorometers were calibrated against chlorophyll *a* measurements (Mantoura et al., 1997) made on cultured algal suspensions and validated against field samples collected close to the instrument mooring during the course of the deployment.

3.4. Statistics of cross-correlation

In the next section different time series will be compared, for example to study relationships

between mixed and shear layer depths and wind stress. Although general cross-correlation statistics like coherency were computed, none of them were found significant at the 95% level of confidence, despite occasional qualitative agreement. This is understood because either 1/ a particular (low-frequency) band was not well resolved to allow proper statistics, for example monthly variations from a 2 months time series, 2/ random statistics were not applicable, 3/ dominant processes were highly nonlinear, so that a single event of good correspondence was indistinguishable in the frequency domain.

4. Observations

4.1. Background information

At the PROVESS site in the northern North Sea currents are dominated by semidiurnal tidal frequencies, with the semidiurnal lunar tidal M_2 major and minor axes averaging 0.186, $0.074\,m\,s^{-1}$, respectively, and semidiurnal solar S_2 0.063, $0.028\,m\,s^{-1}$. These current speeds are responsible for a frictional bottom boundary layer of about 30 m height above the bottom, during springs. Occasionally, motion was enhanced at f, reaching a magnitude of about $0.15\,m\,s^{-1}$. Periods of enhanced energy at f were associated with enhanced wind stress rotation, as modeled by Knight et al. (2002) essentially using Pollard and Millard's (1970) slab layer model. During the first month of observations the weakly stratified near-surface was little affected by wind mixing, as wind speeds seldom exceeded $15\,m\,s^{-1}$. In contrast, during the second month of observations a continuous sequence of storms past the moorings and the pycnocline deepened accordingly.

4.2. Observing a reducing pycnocline in autumn

During the two months period of observations the reduction of stratification was observed in different ways (Figs. 3 and 4). Until about September 29 (day 272), the surface temperature remained approximately constant (Fig. 4c) and until day 260 little occurred near the relatively thick layer of enhanced stratification (Fig. 3a). Within the pycnocline, the largest stratification was observed immediately below the weakly stratified near-surface layer (reaching down to h_s). The weakly stratified near-bottom layer (reaching up to h_b) did not extend higher than about 35 m above the bottom, slightly higher than expected from Ekman dynamics applied for tidal friction (30 m).

The surface temperature decreased with time due to atmospheric induced mixing, h_s reached deeper, h_b shallower and the pycnocline thickness D decreased, along with stratification. Towards the end of the observations a relatively thin, sharp pycnocline resulted. On the large (monthly) time scale, D decreased with time like the overall temperature difference. On shorter time scales of a few days, D varied strongly with time (Fig. 4c), sometimes related to wind stress variation (Fig. 4a). (Wind stress also affects currents, which may become affected by stratification in turn.) The strongest current-stratification effects were not necessarily related to strong wind stress, for example near day 265 when the dominating spring-neap tidal current cycle was broken within the pycnocline (Fig. 3b).

Spring tidal currents occurred near days 265, 280 and 295, but only between days 270 and 290 was the familiar spring-neap cycle observed from surface to bottom in the unfiltered current magnitude data. Especially between days 263 and 267 and days 288 and 298, a modulation was

Fig. 3. Time-depth distribution of stratification observed in different ways in the northern North Sea in autumn, 1998. (a) Classical measure for stratification N^2 from unfiltered temperature gradient data measured by the thermistor string as in Eq. (2) using Eq. (1). Solid lines indicate depths of weakly stratified near-surface (h_s) and -bottom layer (h_b) as in Eq. (6). For reference, these lines are repeated in all panels. (b) Current magnitude $|\mathbf{U}| = (u^2, v^2)^{0.5}$ from the unfiltered data measured by the bottom-mounted 150 kHz ADCP. (c) Shear magnitude squared computed from the ADCP data. The coloring per unit is the same as for N^2. (d) ADCPs echo intensity data (I) with reference to a corrected minimum value (I_0) at each (of 23) depth cell levels. The vertical dashed lines in all panels indicate events described in the text, from left to right: first period of strong inertial shear in the record (day 263), start of autumnal decreases of surface temperature (272), first prolonged period of $Ri<1$ (292).

observed with a period of 4.5–5 days, ranging from almost doubling to almost annihilation of near-surface and, in anti-phase, of pycnocline or near-bottom currents. These periods were characterized by enhanced inertial motion whose frequency differed by less than 1% from the local inertial

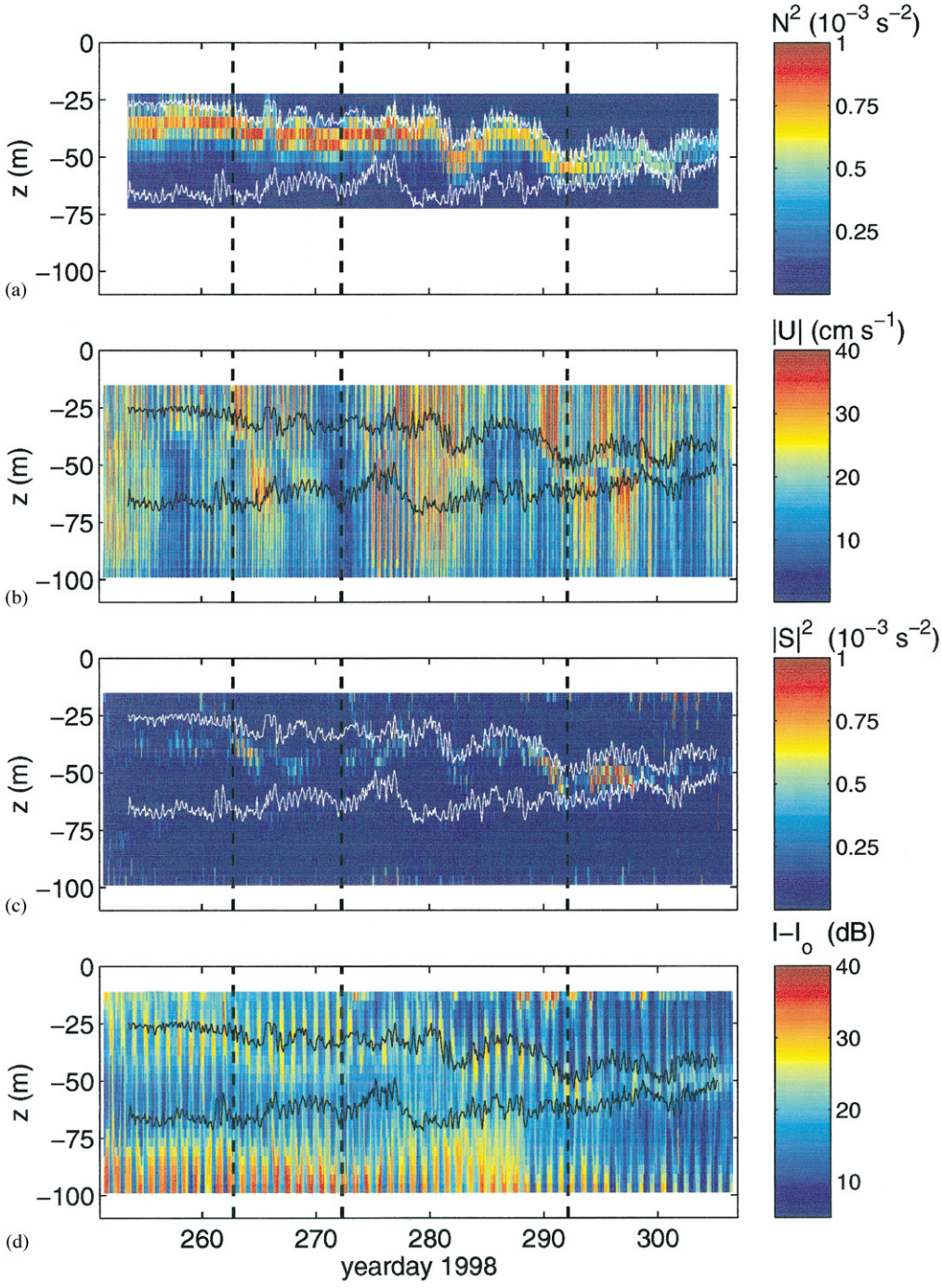

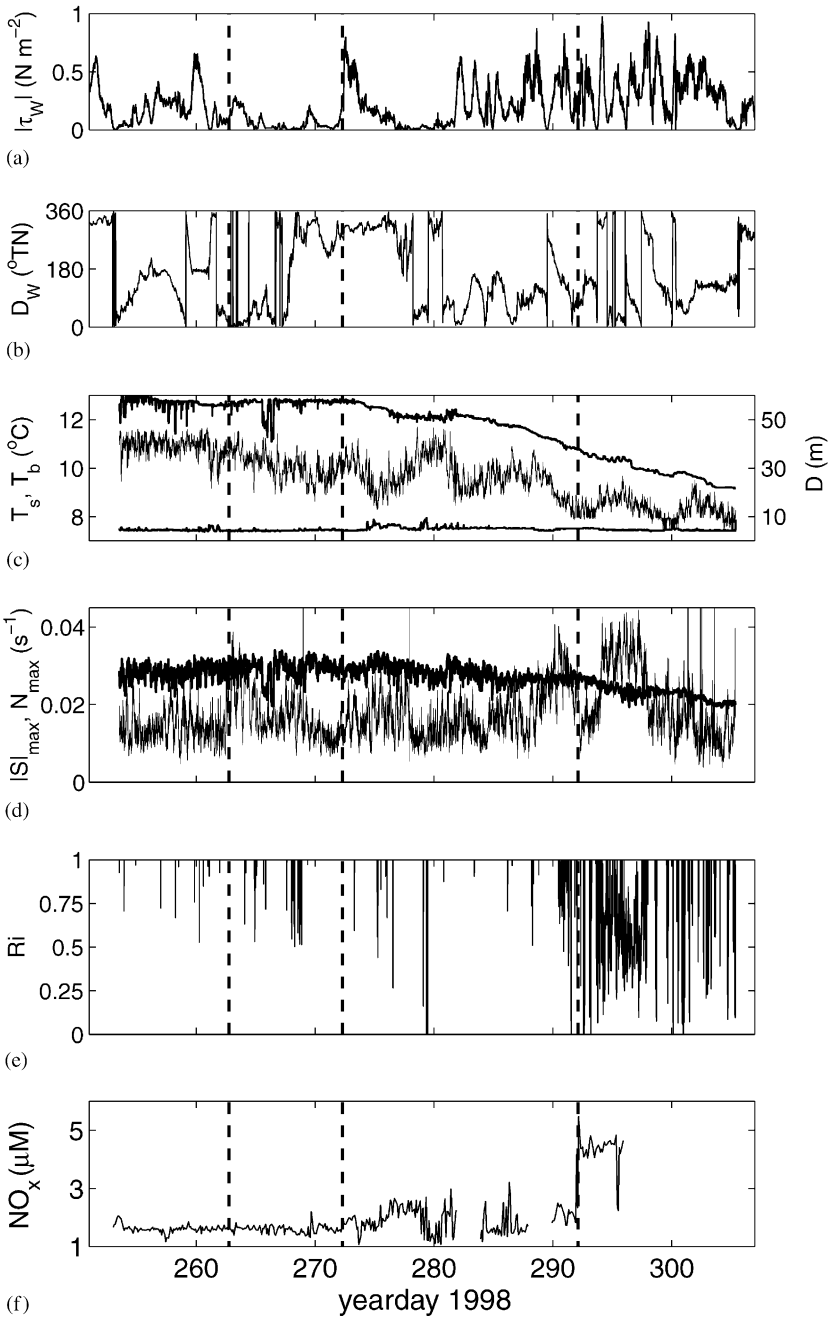

Fig. 4. (a) Wind stress magnitude, (b) wind direction (oceanographic convention), measured at oil rig 'Frigg'. (c) Temperature measured at 30 and 107 m depth (thick lines) and pycnocline thickness (D from Eq. (6); central thin line, scale to the right). (d) Maximum values per time interval of stratification (N_{max}; thick line; weak variation with time) and shear magnitude ($|\mathbf{S}|_{max}$; thin line). (e) Richardson number from Eq. (3) from the thermistor string and ADCP data at 56 m depth, where the largest shear is found. (*f*) Nitrate and nitrite measured at 3 m below the surface. In all panels vertical dashed lines as in Fig. 3.

frequency (Knight et al., 2002). The beat period between f–M_2 (the semidiurnal tidal lunar frequency) is 4.77 days.

This pattern of inertial-tidal modulation is similar to that observed in the central North Sea in summer (van Haren et al., 1999), including the strong baroclinic mode-1 ($j = 1$) appearance of the inertial motions, the tidal currents being mainly barotropic. As in the central North Sea, the maximum amplitude of the near-inertial currents was just less than that of the local barotropic semidiurnal tidal currents ($A_f/A_{M2} \approx 0.7$).

Except for the first period when the wind stress was extremely low, Knight et al. (2002) were able to mimic reasonably the onset of observed inertial motions. Similar to the models used by Millot and Crépon (1981) and Krauss (1981) they included a coastal boundary condition, but we note that our mooring site is just further than one external Rossby radius from the coast. Curiously, a barotropic response at the coast yields the interior quasi-baroclinic ($j = 1$) response for inertial motions. We resume in Section 5 (Discussion), and use the result here of maximal shear across stratification, as both current components are observed 180° out-of-phase, shear being abruptly generated within an inertial period (van Haren, 2000).

Apart from some shear due to wind stress enhancement near the surface in the second half of the record, shear was largest near mid-depth but its magnitude (Fig. 3c) appears to have varied more strongly with time than with stratification (Fig. 3a). Largest shear magnitudes were observed during periods of enhanced inertial motion, and only then did the value of (maximum) shear exceed the value of (maximum) stratification (Fig. 4d). Inertial shear magnitude persisted much longer than an inertial period, as inertial shear (Fig. 5) showed circular anti-cyclonic polarization implying a "constant" magnitude.

These observations compare *and* contrast with those from the central North Sea, where due to the proximity of bottom tidal friction the shear was almost continuously in equilibrium with stratification in a marginal dynamically stable state (van Haren et al., 1999). In the northern North Sea such

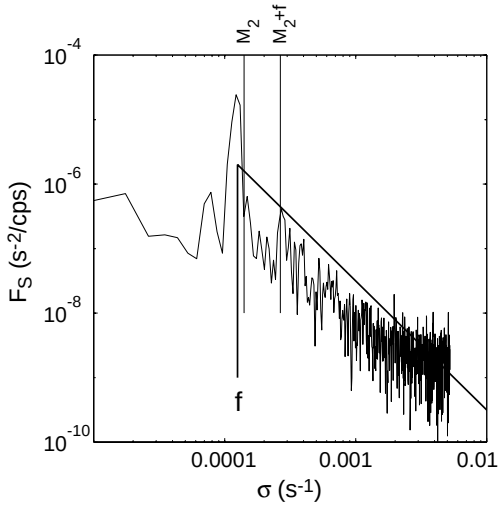

Fig. 5. Shear spectrum from unfiltered 150 kHz ADCP data observed at 56 m depth in the pycnocline between days 290 and 299.

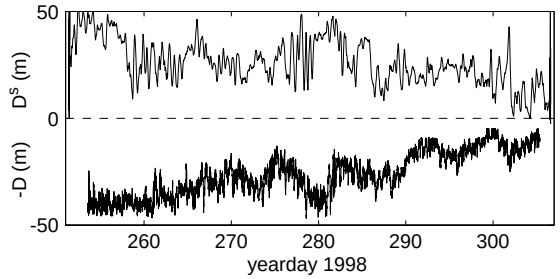

Fig. 6. Comparison between layers of enhanced stratification ($-D$) from Eq. (6) and shear (D^s) from Eq. (7).

equilibrium was less often found, but shear was observed to be largest where stratification was largest (just below the weakly stratified near-surface layer). Also, we find some qualitative resemblance between the layer thickness of stratification (D) and shear (D^s) (Fig. 6), when transition values are used as in Eqs. (6) and (7), respectively. A marginal dynamically stable state implies occasional mixing across stratification, but firstly we resume with the observation of enhanced bottom boundary layer contributing to the reduction of D, D^s.

4.3. What determines the height of a bottom boundary layer?

In a tidally dominated shelf sea the height of the weakly stratified bottom boundary layer is determined by the weighted average of the frictional Ekman depths of the two rotary current components at the semidiurnal tidal frequency (van Haren, 2000). In most cases the anticyclonic (clockwise) Ekman depth $\delta_- = \sqrt{2A}/|\sigma - f|$, A eddy viscosity and σ frequency, is largest. However, in the northern North Sea this does not reach more than about 30 m above the bottom during spring tides, so that the sharpest pycnocline is not reached, as observed. Nevertheless, h_b is observed to increase with time, while the pycnocline is still finitely thick and direct exchange with the weakly stratified surface layer cannot occur. Assuming that frontal advection is unimportant, two possibilities are suggested for pycnocline erosion from below.

The direct effect is the generation of a (surface) wave bottom boundary layer. Despite the water depth and persisting stratification, enhanced surface wave height H_s bears resemblance at times with enhanced h_b, provided a time lag of 1–2 days is invoked (Fig. 7). This resemblance is not statistically significant over the full time series record. Such direct surface wave action causes the bottom to be reworked, which indeed happened between the deployment and recovery of the moorings (Fig. 8). The indirect effect is through generation of near-inertial motions so that current magnitude increases, but more importantly because δ_- becomes very thick when $\sigma \to f$.

However, such a hypothetical situation seldom occurs and near-inertial motions exhibit a finite Ekman depth when low-frequency (sub-inertial) relative vorticity ($\langle\omega\rangle = \langle v\rangle/\partial x - \partial\langle u\rangle/\partial y$) is nonzero (Maas and van Haren, 1987), rendering an effective inertial frequency $f^* = f + 0.5\langle\omega\rangle$ (Kunze and Sanford, 1984) and effective Ekman depth $\delta^*_-(f^*, \sigma)$. As a result, a near-inertial frictional boundary larger (smaller) than the tidal boundary layer is expected when horizontal current differences are smaller (larger) than $O(0.7 \times 10^{-6}\,s^{-1} \approx 0.07f)$. Such horizontal current shear is not uncommon, especially in density fronts and considering local bottom topography. Given the lack (or delayed response) of a relationship between periods of enhanced h_b and inertial motions, this reasoning implies relatively large low-frequency vorticity of $|\langle\omega\rangle| \approx 0.1f$ so that the *tidal* bottom boundary becomes enhanced by $\delta^*_-(f^*, M_2) \approx 1.5\delta_-(f, M_2)$, and the pycnocline may become eroded from below.

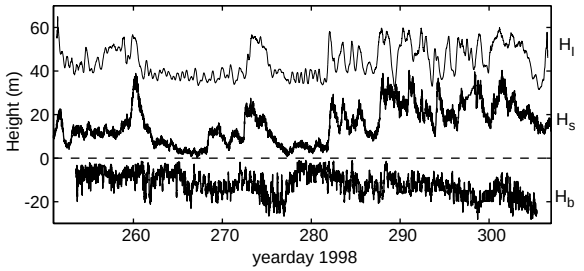

Fig. 7. Weakly stratified near-bottom boundary layer height (h_b; lower graph, indicating -(h_b−30) (m) with surface wave height (H_s; middle graph, indicating H_s-10 (10^{-1} m), measured at Frigg and inferred from near-surface echo intensity data (H_{Ia}, four-hourly smoothed; upper graph, indicating H_{Ia} + 20 (10^{-1} m). Note the qualitative correspondence between both sets of wave 'observations' using the parametrization $H_{Ia} = 10^{0.024Ia-0.13}$, I_a in dB. This is very close to the parametrization in van Haren (2001) for a 600 kHz ADCP. Surface wave action is also generating turbulence at the bottom in addition to tidal friction. A weak relationship can be observed, when a time-lag of about 1–2 days is allowed, h_b lagging the waves.

4.4. Mixing across a pycnocline

Direct evidence for mixing across the *entire* layer of enhanced stratification near mid-depth is lacking. Over the deployment period, the near-bottom temperature remained constant or even decreased slightly with time, indicating that exchange with warmer near-surface water probably did not occur. However, considering the variability of the bottom temperature with time (Fig. 4c), horizontal advection may obscure vertical exchange and other observed quantities point to vertical exchange across (parts of) enhanced stratification.

Destabilizing maximum shear was observed related to D (Fig. 4c and d), to such an extent that D seemed to decrease as shear increased until day 292, but became in-phase when inertial shear

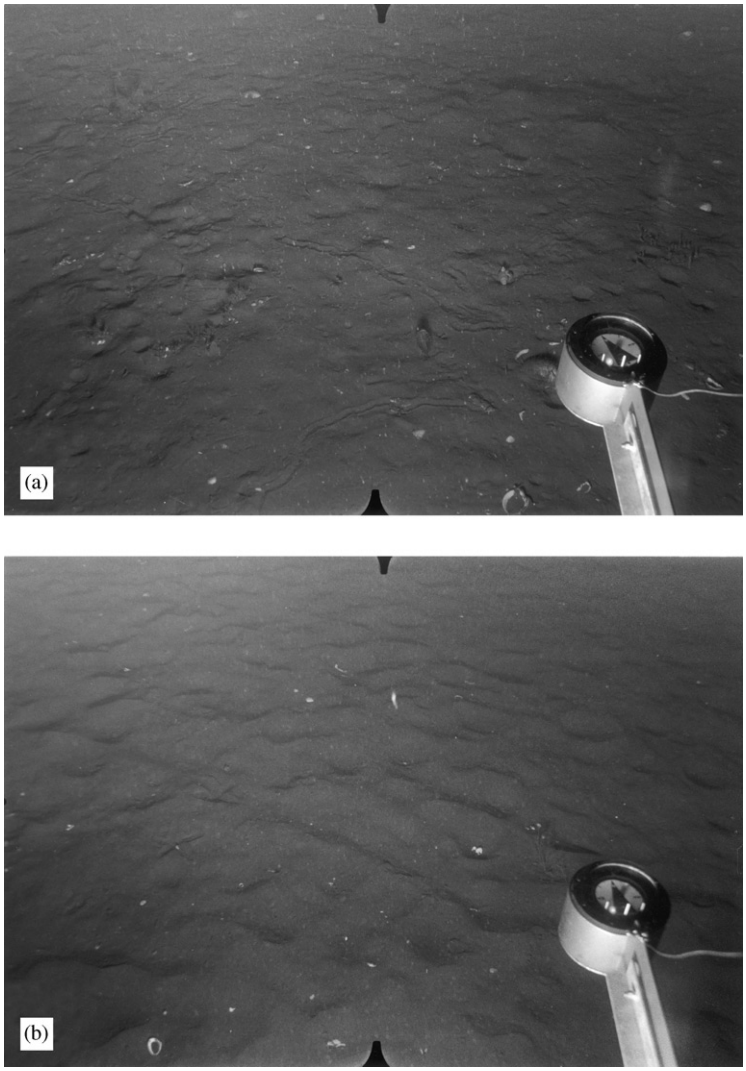

Fig. 8. Bottom structure. (a) Reworked bottom by benthic activity observed on day 258, and (b) completely eroded bottom with wave activity evidence by ripples on day 309.

was largest (between days 294 and 297). The latter qualitative similarity between D and D^s has correspondence in the Richardson number (Fig. 4e). Despite an unknown uncertainty in computed Ri using data sampled 5 km apart and not at the same depth (intervals), results seem firm as minimum Ri is found during maximum shear. This corresponds with observations in the central North Sea in summer (van Haren et al., 1999), including a similar slope $\gamma \approx 0.15 < Ri_{\min}(= 0.25)$, $|\mathbf{S}|^2 = \gamma N^2 + \text{constant}$.

Most striking is the first prolonged period of time from day 292 onward when $Ri < 1$ occurred as a layer of enhanced inertial shear passed the sensors (Fig. 4e). During this period values of diffusivity up to $K \approx 10^{-3}\,\mathrm{m^2\,s^{-1}}$ are inferred in the pycnocline from CTD observations (Fig. 9), with a mean value $\langle K \rangle = 2.7 \pm 1.0 \times 10^{-4}\,\mathrm{m^2\,s^{-1}}$ between days 295–300 ($N > 0.07\,\mathrm{s^{-1}}$). These values are larger by two orders of magnitude than those observed around days 255–260, when stratification was strongly affected by interleaving, which is less

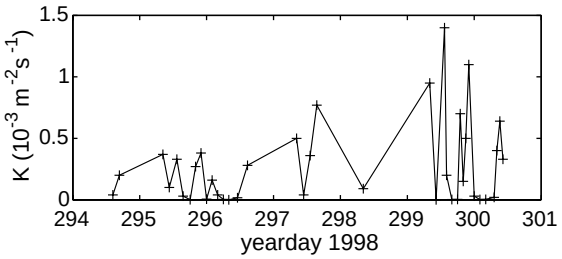

Fig. 9. Eddy diffusivity according to Eq. (8), using raw CTD profiles. Each point indicates the mean value per profile at depths where stratification is large ($N(z) > 0.006\,s^{-1}$).

important in the CTD observations made between days 295 and 300. These values are also larger by an order of magnitude than those estimated in summer in the central North Sea, and than attributed to internal wave breaking in the deep ocean. This amount of turbulent exchange across stratification is supported by the sudden enhancement of nutrients near the surface at day 292 (Fig. 4f), which must come from the pycnocline or below. No large horizontal gradients in surface layer nutrients were observed that could explain the enhancement in the time series record.

The record of in situ nutrient data needs some explanation. Considering the time series of the onboard standard data and the record of the blanks the NAS delivered a reasonably good time series of in situ nutrients. However, there were three periods of about three days duration each in the record when both the in situ nutrients and the onboard standard data showed strong high-frequency variability. These data were due to poor performance of the instrument and therefore are not trustworthy. They were left out from Fig. 4f. The jump at day 292 is real.

This doubling of the amount of nutrients in the surface layer follows shortly after the pycnocline thinned to less than 10 m (within one thermistor depth difference), which was achieved by the surface layer deepening during enhanced inertial shear. Surprisingly, little or no response to the nutrient increase was observed in the near-surface chlorophyll, a measure for phytoplankton biomass (Fig. 10). In contrast earlier, during storms (days 273, 281) and convection (day 276), occasional low *Ri* was associated with a weak enhancement of

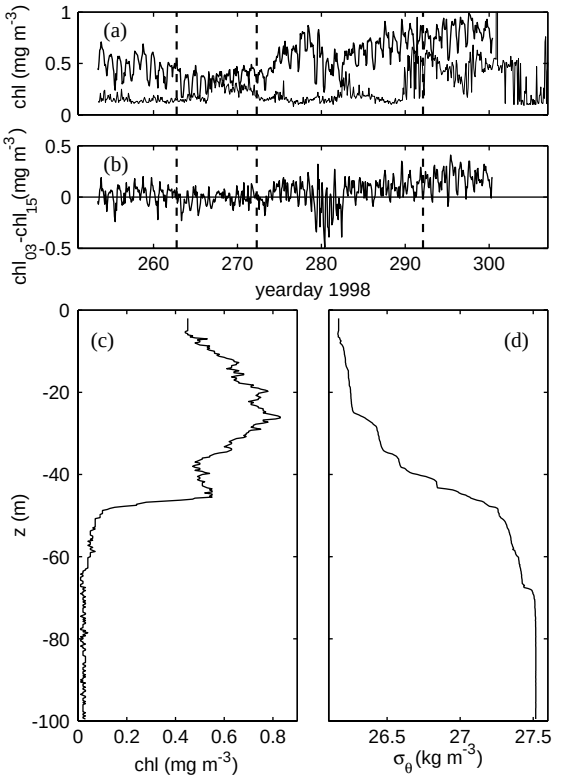

Fig. 10. (a) Time series of phytoplankton biomass in terms of chlorophyll-a inferred from calibrated in situ fluorescence observations at 1.5 (thick line) and 60 m depth (thin). Vertical dashed lines as in Fig. 3. (b) Difference between chlorophyll-a observed at 1.5–15 m depth. (c) Vertical profile of chlorophyll-a from calibrated fluorometer data observed close to the ADCP mooring site at day 254.44. (d) Simultaneously obtained vertical profile of density anomaly.

nutrients together with a phytoplankton increase in the weakly stratified near-surface layer (Figs. 4f, 10). We suggest the following explanation for the observed different responses of phytopankton and nutrients to environmental turbulence and stratification conditions.

The immediate increase of the near-surface chlorophyll following enhanced mixing is most likely attributable to mixing of the standing stock of phytoplankton in the near-surface layer, as largest phytoplankton amounts are found in weakly stratified layers *above* the main pycnocline (Fig. 10c,d). Apparently, nutrients are enhanced at that level too, and mixed simultaneously with the

phytoplankton (compare Figs. 4f and 10a). Note also that after day 270 variations with time of phytoplankton biomass observed at ~ 60 m depth are all related to moments when $|h_s| > 45$ m, including the relatively large increase at day 290 and the subsequent decrease at day 300, when the pycnocline rose again.

This response appears to be different from nutrient and phytoplankton observations in the central North Sea in summer, where a delay of about 9 days was observed between nutrients and phytoplankton increase (Fig. 3 in van Haren et al., 1999), implying growth at the depth of observations. Speculating, the lack of local growth response to the sudden nutrient increase observed in the northern North Sea at day 292 could be due to light limitation of algal growth due to shorter day length and greater mixing depth or, alternatively, due to premature cessation of the observations, on day 299.

Additional evidence of exchanges between the weakly stratified near-bottom and near–surface layers was anticipated from the ADCPs echo intensity data (Fig. 3d), as a measure for *unspecified* suspended material subject to vertical exchange of mass. However, considerably less of such evidence is available in these data. Clearly from Fig. 3d, echo intensity data are less suitable for detection of ranges of enhanced stratification, despite the change in density and associated refraction of acoustic beams (Gordon, 1996). Apparently, the dominant scatterers in the northern North Sea are independent of stratification, and the relative proximity of surface and bottom are more important.

Most conspicuous in the echo intensity data is the diurnal signal, as has been reported in the literature so often before, and attributed to the vertical migration of zooplankton, hiding deeper in the water column during daytime. Two regions of enhanced echo intensity are observed likely related with zooplankton abundance, one more or less following h_s and occupying the pycnocline after day 290, the other occupying the weakly stratified near-bottom layer. Tentatively, zooplankton seem to decrease with time, as the amplitude of (this diurnal variation in) echo intensity decreases with time, including a sudden halt at day 288 near the bottom. Broadly, three weak echo intensity regions can be designated, one in the near-bottom layer after day 288, the second between 50 and 75 m depth between days 255 and 290, and the third in the weakly stratified near-surface layer after day 282.

The last weak echo intensity region corresponds to periods when phytoplankton were increasing, perhaps indicating an increase of phytoplankton stock due to lack of grazing (in addition to nutrient supply). Note also that the large echo intensity values near the layer of strongest stratification are associated with the *lowest* phytoplankton values (Fig. 10). As echo intensity does not seem to represent phytoplankton, it also does not seem to represent suspended sediment properly (or other suspended material to which optical instruments are sensitive), because low turbidity values have been observed at the depth of largest stratification between days 294 and 300 (Jago et al., in press). This may explain the rather unusual near-bottom observations in Fig. 3d.

If echo intensity has some relationship with suspended sediment one would expect a relation with the amount of turbulent friction in the near-bottom layer. Indeed one can only observe indications of a spring-neap cycle with difficulty and below 80 m depth (recall that spring tide is near day 280). As a result, besides a loss of zooplankton the sudden decrease in near-bottom echo intensity may indicate a loss of suspended material following strong erosion attributable to enhanced wind stress from day 282 onwards.

As in the near-surface layer entrained air bubbles designate periods of enhanced wind and waves, there is sometimes a corresponding response near the bottom (day 274) and sometimes there is not (day 291). Largest near-bottom echo intensity values are found not necessarily related with rough weather or spring tide: between days 267 and 272, and 284 and 288, when enhanced echo intensity values reach up to h_b.

5. Discussion

In addition to direct near-surface mixing induced by wind stress and convective overturning,

our observations from the northern North Sea confirm earlier studies (Krauss, 1981; van Haren et al., 1999) about the importance of inertial motions on the reduction of stratification in autumn, although details are different.

Inertial motions generate largest shear at the depth of largest stratification, to such an extent that the water column becomes marginal dynamically stable. As the inertial frequency is the lower frequency bound of internal gravity waves, it is suggested that such low-frequency internal wave shear causes mixing within the pycnocline through occasional breaking of high-frequency internal waves. The latter are generated by nonlinear processes, of which enhanced levels at coupling frequencies like M_2+f are evidence (Fig. 5a). Observations presented here partially confirm this picture as a relatively high turbulent diffusivity of $0.5–1\times10^{-4}\,m^2\,s^{-1}$ was found when inertial shear was large, which persisted for several days.

However, despite the slow variation with time of the inertial shear magnitude, generation and attenuation of inertial shear may occur very abruptly. The (mis)-match between the phase of the near-surface inertial motion and the passing atmospheric disturbance seems to be an important property. This can be modeled relatively easily to obtain inertial motions in the weakly stratified near-surface layer. As already indicated by Krauss (1981), inertial motions below the layer of enhanced stratification and, therefore, inertial shear, are more difficult to model. This is partially due to the relative importance of properly modeling pycnocline thickness, which is controlled via Richardson number, like density and velocity difference.

Another reason is that it is not well understood why inertial motions exhibit a mode-1 vertical structure, with 180°-phase difference for both current components across the largest stratification. Like Millot and Crépon (1981) and Krauss (1981), Knight et al. (2002) modeled this problem by invoking a coastal boundary condition, which is also justified for our mooring site relatively far from the coast as follows.

The near-surface response is generated simultaneously near the coast and the mooring site (250 km away). Furthermore, the near-surface Ekman transport sets up a pressure gradient perpendicular to the coast, generating a response so that the current below the stratification is 180° out-of-phase. This barotropic response is communicated to the interior at phase speed $\sqrt{gH}\approx30\,m\,s^{-1}$ reaching the mooring site within $t\approx1/f$, yielding an additional phase difference between surface and bottom of about 60°. Considering the sensitivity of inertial to (vertical variations in) viscosity, this phase difference is smoothed away as has been proven for tidal currents (van Haren, 2000), so that at least one current component is 180° out-of-phase across the pycnocline, where viscosity is reduced. Once thus established, this renders *both* current components 180° out-of-phase, as inertial motions are circularly polarized, by nature.

Much later in time when the baroclinic wave is set up the above barotropic-viscous model should be replaced by an (inviscid) model (for instance, Millot and Crépon, 1981) that generates a baroclinic (mode-1) inertial interfacial wave. Such model is not considered here.

6. Conclusions

A clear view is obtained of the autumnal erosion of a well-defined stratification in a moderately deep (~100 m) shelf sea. In contrast with shallower seas, where frictional stresses from surface and bottom approach closely, and in contrast with the deep ocean, such moderately deep shelf sea is characterized as follows. The erosion of stratification occurs by atmospheric mixing from above *and* by enhanced bottom friction from below. Enhanced mixing across stratification occurs when *in addition* inertial shear is generated.

Furthermore, it is shown that,

- Enhanced surface wave action has little effect on stratification while reworking the bottom.
- Shear is largest where largest stratification is found, confirming shear being the next best indicator for stratification after direct observations of density variations. This holds also in areas where tidal shear is not directly affecting stratification.

- Echo intensity data are not a very good indicator for stratification, as too many unknown quantities contribute to this signal.
- Assuming inertial shear (magnitude) acts primarily on large scales >10 km and varying on time scales much slower than the inertial period, (indirect) evidence of such exchange could be monitored well using measurements from moorings 5 km apart.
- As a result of this exchange across enhanced stratification, nutrients are observed suddenly enhanced in the weakly stratified near-surface layer.
- Phytoplankton are observed to increase with time, primarily due to mixing standing stock and not due to local growth, but our records may have been too short to firmly conclude the latter.

Acknowledgements

The assistance of the crews of the R/V Valdivia, R/V Pelagia and R/V Challenger is highly appreciated. Assistance of Joyce Boyd (SOC, Southampton) with deployment and calibration of in situ nutrient analysers is highly appreciated. John Humphery provided the photographs of Fig. 8. Processes of Vertical Exchange in Shelf Seas (PROVESS) is a MAST3 project funded in part by the Commission of the European Communities Directorate General for Science and Education, Research and Development under contract # MAS3-CT97-0159. The PROVESS project was supported in part by the NERC CCMS DYME Programme. This is also NIOZ-contribution 3677.

References

Brainerd, K.E., Gregg, M.C., 1995. Surface mixing and mixing layer depths. Deep-Sea Research I 42, 1521–1543.

Gordon, R.L. 1996. Acoustic Doppler current profiler, Principles of operation, A practical primer. RDI, San Diego, 51pp.

Hill, A.E., Souza, A.J., Jones, K., Simpson, J.H., Shapiro, G.I., McCandliss, R., Wilson, H., Leftley, J., 1998. The malin cascade in winter 1996. Journal of Marine Research 56, 87–106.

Jago, C., Jones, S.E., Latter, R.J., McCandliss, R.R., Hearn, M.R., Howarth, M.J. Resuspension of benthic fluff by tidal currents in deep stratified waters, northern North Sea. Journal of Sea Research, in press.

Knight, P.J., Howarth, M.J., Rippeth, T.P., 2002. Inertial currents in the northern North Sea. Journal of Sea Research 47, 269–284.

Krauss, W., 1981. The erosion of the pycnocline. Journal of Physical Oceanography 11, 415–433.

Kunze, E., Sanford, T.B., 1984. Observations of near-inertial waves in a front. Journal of Physical Oceanography 14, 566–581.

Linden, P.F., 1979. Mixing in stratified fluids. Geophysical Astrophysical Fluid Dynamics 13, 3–23.

Maas, L.R.M., van Haren, J.J.M., 1987. Observations on the vertical structure of tidal and inertial currents in the central north sea. Journal of Marine Research 45, 293–318.

Mantoura, R.F.C, Wright, S.W., Jefferey, S.W., Barlow, R.G., Cummings, D.E., 1997. Simple isocratic HPLC methods for chlorophylls and their degradation products. In: Jefferey, S.W., Mantoura, R.F.C, Wright, S.W. (Eds.), Phytoplankton pigments in Oceanography: Guidelines to Modern Methods. UNESCO Paris, France, pp. 307–326.

Miles, J., 1987. Richardson's number revisited. In: Preprints of 3rd Intl. Symposium on Stratified Flows, CalTech, Pasadena, CA, February 3–5, pp. 1–7.

Millot, C., Crépon, M., 1981. Inertial oscillations on the continental shelf of the Gulf of Lions-Observations and theory. Journal of Physical Oceanography 11, 639–657.

Pollard, R.T., Millard Jr., R.C., 1970. Comparison between observed and simulated wind-generated inertial oscillations. Deep-Sea Research 17, 813–821.

Pollard, R.T., Rhines, P.B., Thompson, R.O.R.Y., 1973. The deepening of the wind-mixed layer. Geophysical Fluid Dynamics 3, 381–404.

Thorpe, S.A., 1987. Current and temperature variability on the continental slope. Philosophical Transactions of the Royal Society of London A323, 471–517.

van Haren, H., 1996. Correcting false thermistor string data. Continental Shelf Research 16, 1871–1883.

van Haren, H., 2000. Properties of vertical current shear across stratification in the north sea. Journal of Marine Research 58, 465–491.

van Haren, H., 2001. Estimates of sea level, waves and winds from a bottom-mounted adcp in a shelf sea. Journal of Sea Research 45, 1–14.

van Haren, H., Maas, L., Zimmerman, J.T.F., Ridderinkhof, H., Malschaert, H., 1999. Strong inertial currents and marginal internal wave stability in the central north sea. Geophysical Research Letters 26, 2993–2996.